RECENT SKYSHINE CALCULATIONS AT JEFFERSON LAB

P. Degtyarenko

Thomas Jefferson National Accelerator Facility, Newport News, VA 23606

(April 24, 1997)

MASTER

New calculations of the skyshine dose distribution of neutrons and secondary photons have been performed at Jefferson Lab using the Monte Carlo method. The dose dependence on neutron energy, distance to the neutron source, polar angle of a source neutron, and azimuthal angle between the observation point and the momentum direction of a source neutron have been studied. The azimuthally asymmetric term in the skyshine dose distribution is shown to be important in the dose calculations around high-energy accelerator facilities. A parameterization formula and corresponding computer code have been developed which can be used for detailed calculations of the skyshine dose maps.

I. INTRODUCTION

The complexity of neutron skyshine radiation calculations has drawn a fair amount of attention in literature from the early publications and up to the present time [1–4]. Both analytical [1] and Monte Carlo (MC) [2] approaches have been successfully used to describe the phenomenon. MC methods, generally more powerful and flexible in describing complex geometries and environments, require large computing resources, but become more attractive and easier to use as CPU power and computer memory become cheaper and more readily available. To be more confident in using MC to solve complicated problems, one needs comparisons with established qualitative and analytical quantitative methods, in simple or general cases. Skyshine calculation is a good example of such a problem, as the series of analytical and MC calculations shows reasonably good agreement and provides opportunities for analytical parameterizations.

At the Thomas Jefferson National Accelerator Facility (Jefferson Lab) we need a reliable set of skyshine calculation techniques to be able to predict and manage effectively the radiological impact of the experiments conducted in three end stations with CW electron beams from the nominal 4 GeV accelerator.

We are using the GEANT/CALOR MC (GCALOR, Ref. [5,6]) in our calculations, so we need to calibrate or benchmark its results against the other methods, so that we can use full-scale MC models with confidence. Another purpose of the present study deals with the problem of azimuthal asymmetry of the neutron skyshine radiation caused by operation of a high-energy particle accelerator. The neutron source term cannot always be assumed symmetric around the vertical axis. If there are fixed-target experiments in the experimental halls

with relatively thin roof shielding, and/or the roofs are not horizontally flat then using the standard azimuthally symmetric approach could lead to underestimating of the skyshine dose in the forward direction, and overestimating it in the backward direction. Thus, in parallel with the testing of the applicability of GCALOR MC, we intended to study the azimuthal asymmetry of the skyshine.

II. CALCULATION METHOD

The model setup chosen was close to the standard for such calculations. The density and composition of soil were taken to be the same as in Ref. [1], and the neutron source was positioned 15 m above the surface of the ground. We found no significant difference between the model of the atmosphere used in [1] and the model using variable density dependent on the altitude. We used the model consisting of the atmosphere layers with the parameters specified in Fig. 1.
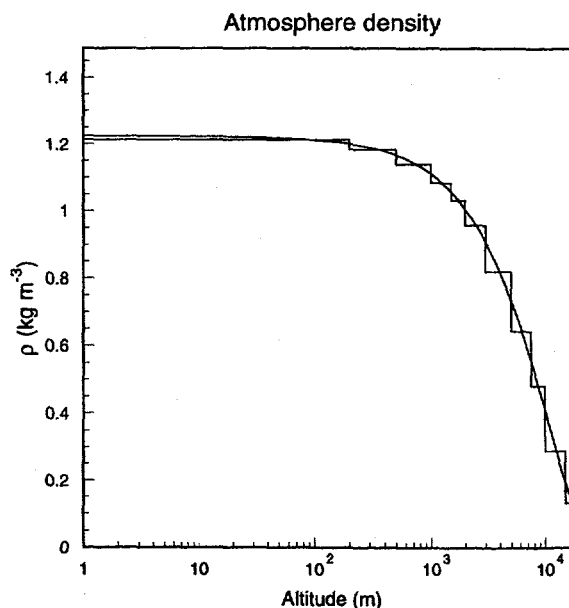
Atmosphere density

FIG. 1. Standard atmosphere density as a function of altitude (curve), and layers of constant density in the GEANT model of the atmosphere (histogram).

The study of the skyshine neutron and photon dose at the ground/air interface was performed systematically in 19 intervals of neutron kinetic energy T_n from thermal to

DISCLAIMER

Portions of this document may be illegible in electronic image products. Images are produced from the best available original document.

DISCLAIMER

400 MeV, and 5 equal intervals in $\cos\Theta_n$, where Θ_n is the neutron emission polar angle relative to the vertical axis, $0 < \cos\Theta_n < 1$. Ten of 19 energy intervals coincided with the energy intervals used in Ref. [1] to allow comparisons; the remaining intervals filled the gaps. Source neutrons were generated and evenly distributed within the T_n and $\cos\Theta_n$ intervals chosen, and then the full cascades of secondary interactions were generated by GCALOR. The scoring technique used all the neutrons and photons entering or exiting the ground to calculate the equivalent n and γ flux at the surface. The surface was binned radially in 42 intervals in the range from 0 to 2 km, and in 9 equal intervals in ϕ, where ϕ is the azimuthal angle between the direction of the neutron momentum and the line from the source position to the point at the surface where the skyshine n or γ is scored. The setup has left-right symmetry with respect to the neutron azimuthal direction.

The dose equivalent was determined from the number of neutrons and photons per unit area crossing the ground surface divided by their direction cosine to the normal to the surface. The resultant fluence was converted to dose equivalent by using the conversion coefficients given in a reference by the U.S. DOE [7].

FIG. 3. Same as Fig. 2, but for the neutron kinetic energy interval 498 keV$< T_n <$743 keV.
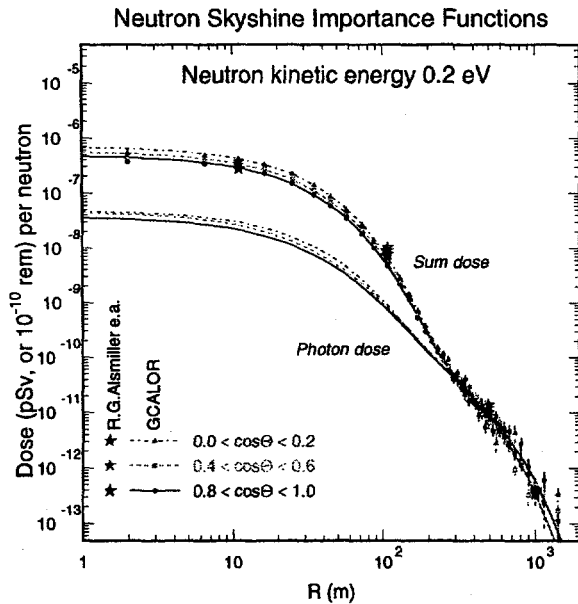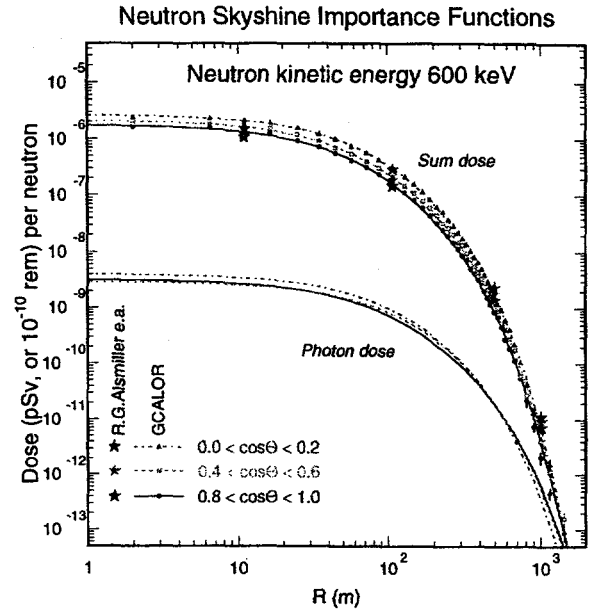

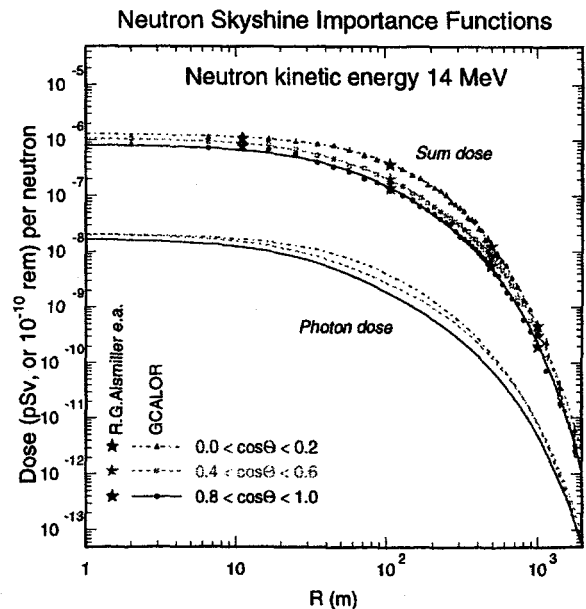FIG. 2. Skyshine dose distribution as a function of radial distance from the source of low energy ($T_n < 0.414$ eV) neutrons. The results of GCALOR calculation are shown by small symbols. Error bars show statistical errors if they are larger than the symbol size. Three intervals in the polar angle of neutron emission are shown using different symbols: circles for close to vertical neutrons emitted at $\Theta \lesssim 37°$, squares for $53° \lesssim \Theta \lesssim 66°$, and triangles for neutrons emitted almost horizontally with $78° \lesssim \Theta < 90°$. Corresponding solid, dashed, and dash-dotted lines represent the parameterization functions. The upper set of lines on top of the calculated values shows the parameterization of the sum (neutron and secondary photon) skyshine dose, $\overline{D}_{sum}(r)$ from Eq. (8). The lower set of lines shows the secondary photon contribution to the sum dose, $\overline{D}_\gamma(r)$ from Eq. (4). The star symbols correspond to the values of neutron skyshine dose calculated in Ref. [1] at four distances in the same angular intervals, for the same interval in T_n.

FIG. 4. Same as Fig. 2, but for the neutron kinetic energy interval 13.5 MeV$< T_n <$ 14.9 MeV.

2

III. RESULTS

The calculated dose distributions, averaged over ϕ, are shown in Figs. 2 to 5, as functions of the radial distance from the source r, in 3 intervals of $\cos\Theta_n$.
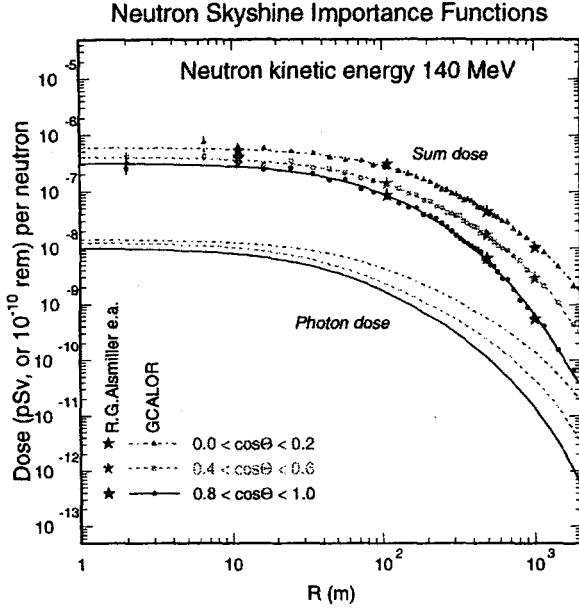

FIG. 5. Same as Fig. 2, but for the neutron kinetic energy interval 125 MeV$< T_n <$150 MeV.

The source neutron kinetic energies chosen for display coincide with the energy intervals of Ref. [1]; agreement is very good in these energy intervals. The comparison in the whole range of neutron energies from thermal up to 400 MeV is given in Figs. 6 and 7 for the two intervals in $\cos\Theta_n$, in 4 intervals on r at each figure. There is a systematic difference between the two calculations in the source neutron energy range from approximately 0.1 keV to 0.5 MeV at large distances, and also some other discrepancies including resonance-like behavior of the difference at $T_n \approx 60 - 70$ MeV, $r = 1005$ m and $\cos\Theta_n = 0.9$. In general, the agreement looks convincing enough to conclude that the GEANT/CALOR Monte Carlo can be used in the skyshine calculations with a good degree of confidence.

Figs. 8 to 11 give an illustration of the calculated ϕ-dependence of the skyshine dose. The ϕ-distributions were accumulated for four radial intervals with mean radii 11, 135, 400, and 1000 meters, in each of 19 × 5 intervals on T_n and $\cos\Theta_n$. The normalization is chosen such that the average value of the ϕ-dependence functions was 1. We may see from the figures that, indeed, the azimuthal asymmetry of the skyshine dose may be important. The most prominent asymmetry is observed in the highest neutron energy interval and at $0 < \cos\Theta_n < 0.2$ when the neutrons are emitted almost horizontally. The difference in the skyshine dose between

the forward and backward directions can reach more than a factor of 1000. The decreasing asymmetry is observed at the $0.8 < \cos\Theta_n < 1$ interval when the setup becomes close to the azimuthally symmetric case, and also at lower energies.
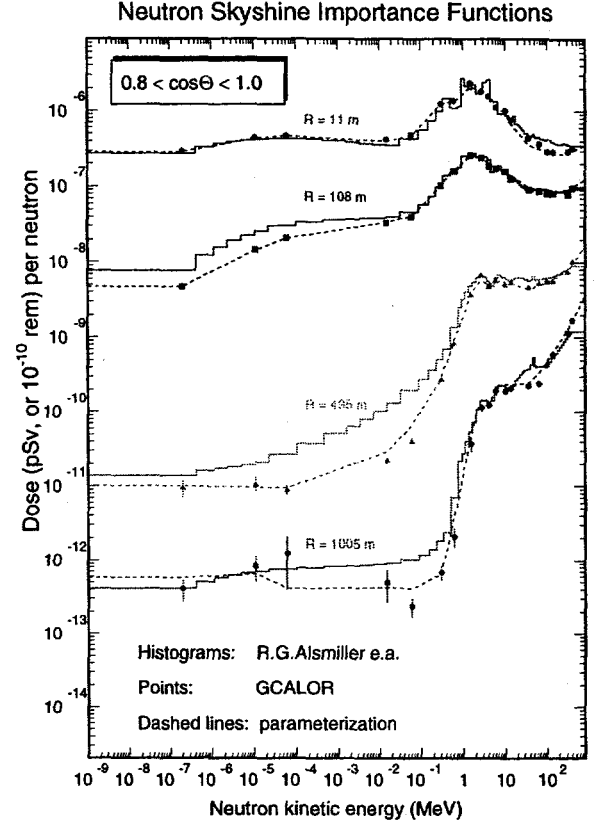

FIG. 6. Skyshine dose distribution as a function of kinetic energy of source neutrons emitted in the angular interval $\Theta \lesssim 37°$. The results of GCALOR calculation are shown by symbols. Error bars show statistical errors if they are larger than the symbol size. Four intervals in the radial distance from the source are shown as different series of points. Histograms correspond to the values of neutron skyshine dose calculated in Ref. [1]. Corresponding dashed lines represent the parameterization functions.

IV. PARAMETERIZATIONS

As a basis for the parameterization of the data we used the fact established earlier in Ref. [2] that the function in Eq. (1) fits well to the calculations for radial distances $r \gtrsim 100$ m:

$$\overline{D}_a(r) = \frac{Q_a}{r} \exp\left(-\frac{r}{\lambda_a}\right), \qquad (1)$$

where a stands for n or γ, Q and λ are parameters, and $\overline{D}_{n,\gamma}(r)$ is the skyshine dose from the neutrons or photons crossing the air/ground interface, averaged over the azimuthal angle ϕ.
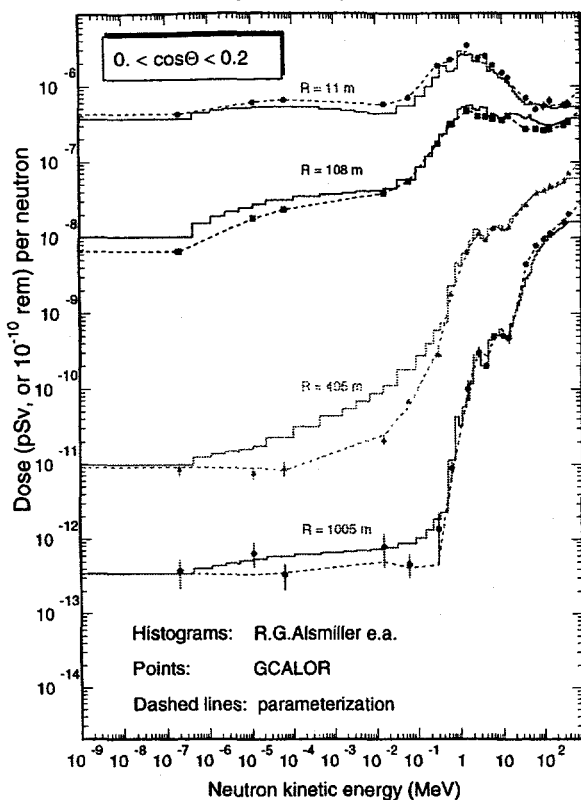
3

Neutron Skyshine Importance Functions

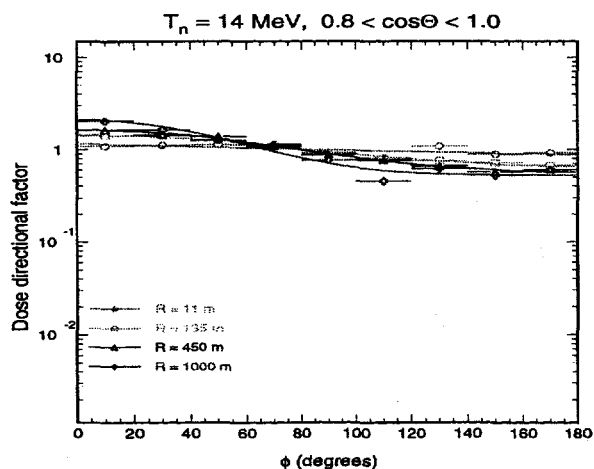FIG. 7. Same as Fig. 6, but for the angular interval $78° \lesssim \Theta < 90°$.

FIG. 8. Skyshine dose directional factors calculated in the $T_n = 14$ MeV and $\cos(\Theta) = 0.9$ interval as a function of azimuthal angle ϕ. Four functions are shown with different symbols corresponding to average radial distances 11 m, 135 m, 450 m, and 1000 m. Corresponding lines represent the parameterization functions $F(\phi)$ from Eq. (5).
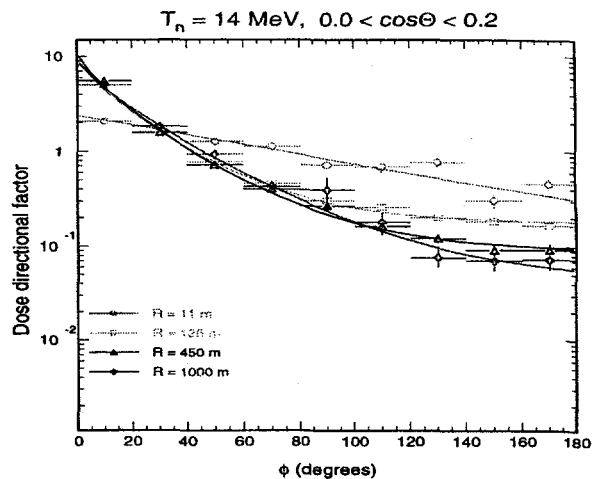

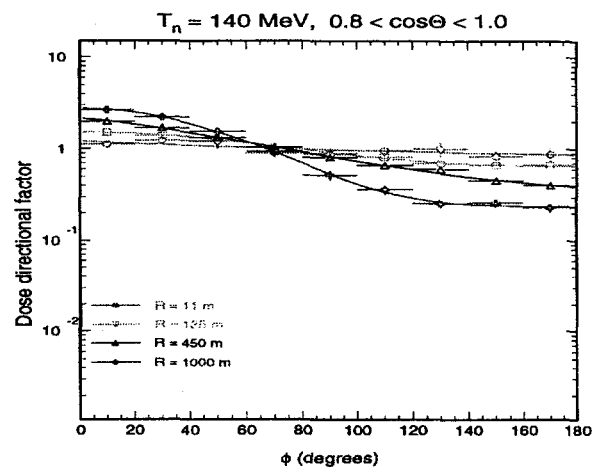FIG. 9. Same as Fig. 8, but for the $\cos(\Theta) = 0.1$ interval.

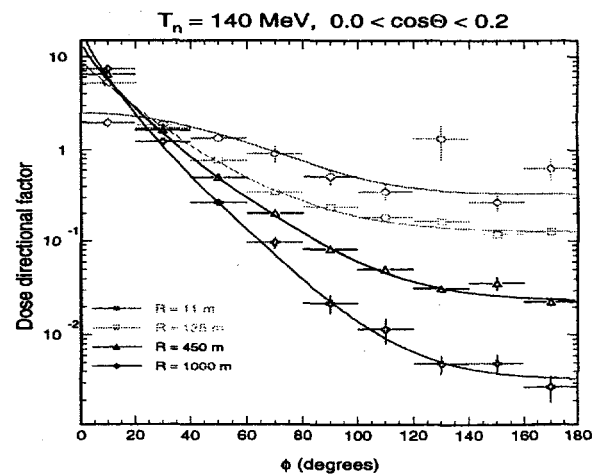FIG. 10. Same as Fig. 8, but for the $T_n = 140$ MeV interval.

FIG. 11. Same as Fig. 10, but for the $\cos(\Theta) = 0.1$ interval.

4

We have found that we can avoid the divergence at small r in the Eq. (1) by using the form

$$\overline{D}_a(r) = \frac{\exp(A_a - B_a r)}{r}\left\{1 - \exp\left[-\frac{C_a r}{\exp(A_a)}\right]\right\}, \quad (2)$$

where parameters A and B correspond to Q and λ, $A_a = \ln Q_a$ and $B_a = \lambda_a^{-1}$, and C_a is an additional parameter, corresponding to the value of the function at small r:

$$\lim_{r \to 0} \overline{D}_a(r) = C_a. \quad (3)$$

The function type Eq. (2) fits very well to the neutron and photon spectra, with the exclusion of several $T_n \times \cos\Theta_n$ intervals. To be able to fit the data as close as possible we introduced two extra parameters (U_a and V_a) keeping the structure of the equation and the meaning of the C_a parameter the same:

$$\overline{D}_a(r) = \frac{\exp(A_a - B_a r) + \exp(U_a - V_a r)}{r}$$
$$\times \left\{1 - \exp\left[-\frac{C_a r}{\exp(A_a) + \exp(U_a)}\right]\right\}. \quad (4)$$

Using Eq. (4) allowed us to parameterize the data very closely; the average χ^2/N fit quality parameter was about 2. The fitting parameters were obtained using the minimization routine MINUIT [8]. The parameterizations are shown in Figs. 2 to 7 as lines.

The azimuthal angle dependences of the type shown in Figs. 8 to 11 were fitted to the equation

$$F(\phi) = f_1\left\{\exp\left[-\left(\frac{\phi}{f_3}\right)^{f_4}\right] + f_2\right\}, \quad (5)$$

where f_1-f_4 are four parameters, with only three being independent due to the imposed condition

$$\frac{1}{\pi}\int_0^\pi F(\phi)d\phi = 1. \quad (6)$$

Thus, the parameterized skyshine dose distributions D_{sum} can be presented in the form of the product of the "regular" (symmetric) skyshine importance function $\overline{D}_{sum}$, and the "dose directional factor" function F:

$$D_{sum}(r, \phi) = \overline{D}_{sum}(r)F(\phi, r), \quad (7)$$

where

$$\overline{D}_{sum}(r) = \overline{D}_n(r) + \overline{D}_\gamma(r). \quad (8)$$

Such fitting procedures were performed in each interval on T_n, $\cos\Theta_n$ and as a result we obtained the parameterization function

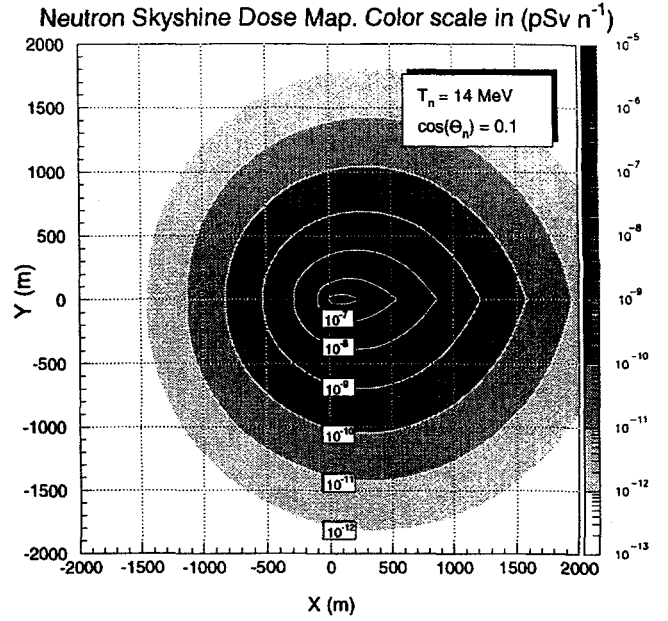$$D_{sum}(r, \phi, T_n, \Theta_n) = \overline{D}_{sum}(r, T_n, \Theta_n)F(\phi, r, T_n, \Theta_n). \quad (9)$$

FIG. 12. Skyshine dose map calculated for the neutrons with fixed kinetic energy $T_n = 14$ MeV and $\cos(\Theta) = 0.1$ using the parameterization function SKYD. Neutron skyshine dose rate distribution around the source point is shown as a color (density) plot with lines of equal dose rate plotted as white contours. The logarithmic color scale for the dose rate is shown as the right scale in the figure; one step in color and the distance between neighboring lines of equal dose rate correspond to a factor of 10 in dose rate. The dose rate in pSv/n is indicated on the labels attached to the white contours.
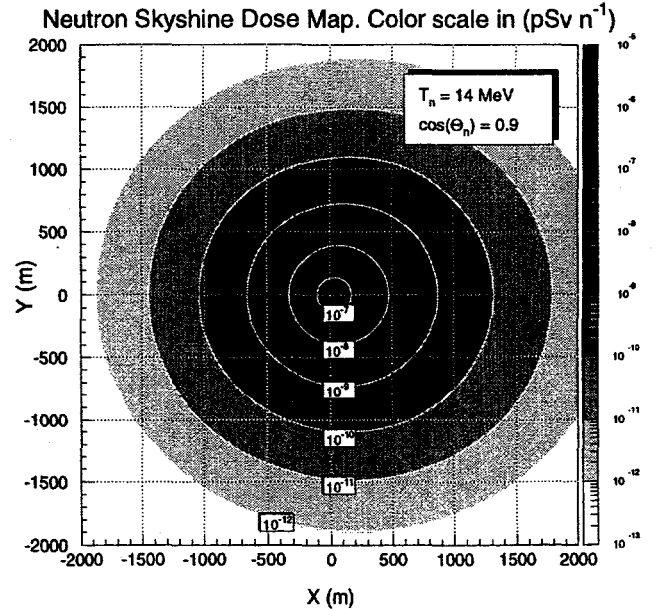

FIG. 13. Same as Fig. 12, but for $\cos\Theta_n = 0.9$.

The FORTRAN subroutine SKYD was developed which reads the parameter files and uses the interpolation

procedures to return the neutron skyshine importance as a function of all the variables including azimuthal direction.

Figures 12 to 15 show the examples of dose maps that can be calculated using the parameterization function, for neutrons of fixed kinetic energy emitted at fixed polar angle. The effects of increasing azimuthal asymmetry are clearly seen at higher energy and the polar angle close to horizontal.
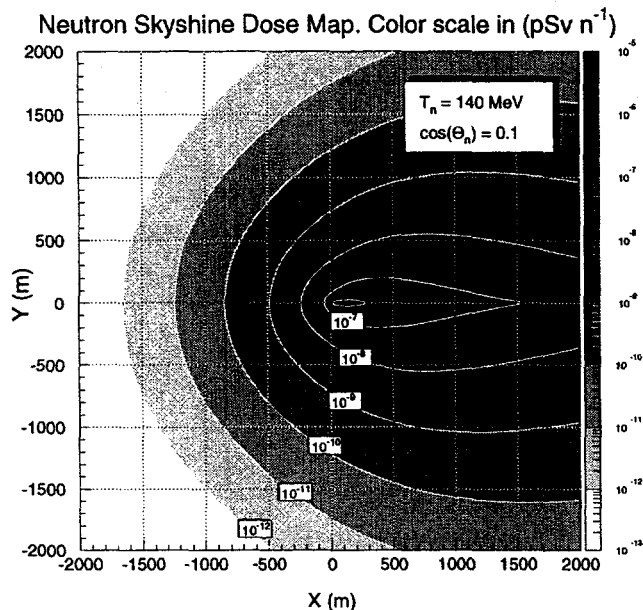

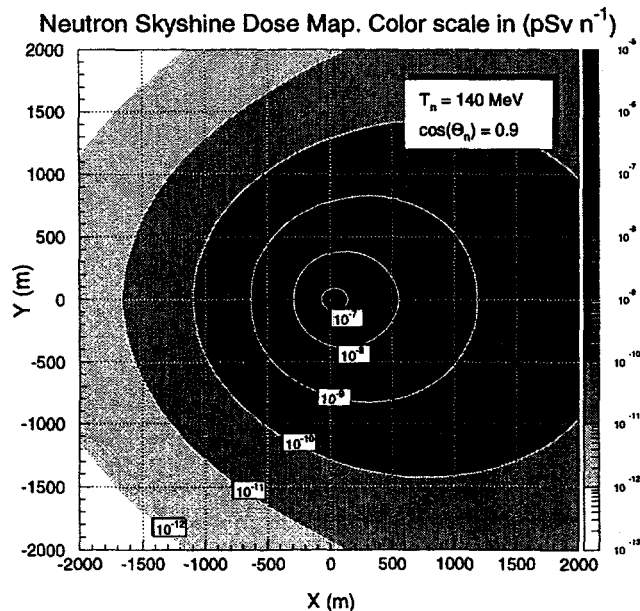FIG. 14. Same as Fig. 12, but for $T_n = 140$ MeV.

FIG. 15. Same as Fig. 14, but for $\cos \Theta_n = 0.9$.

The application of this procedure to the solution of a skyshine problem at Jefferson Lab is illustrated by Fig. 16. GEANT was used to model the experimental setup including target and beam line structures inside the experimental end station building. The beam line and the target are not centered in the hall. The electron beam line is shifted by ≈ 5 m from the central diameter of the hall, as indicated in the figure; the target is also shifted by ≈ 5 m upstream from the middle point of the beam line in the hall. This makes the problem azimuthally asymmetric from the beginning.
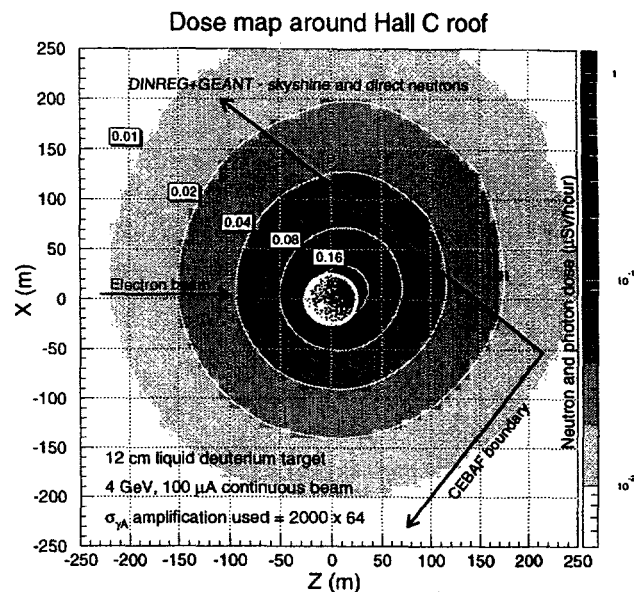

FIG. 16. A schematic map of Hall C and the surrounding CEBAF site is shown. The coordinates: the z-axis is parallel to the direction of the electron beam entering the hall as indicated by the arrow; the $x - z$ plane is parallel to the ground surface; the y-axis is vertical. The hall is shown in the center of the figure as a white circle. The corner of the CEBAF site boundary nearest to the hall is shown by the two arrows. The $x - z$ coordinate distribution of neutrons exiting the hall roof is illustrated by a scatter-plot on top of the hall circle. The neutron skyshine dose rate distribution around the hall is shown as a color (density) plot with lines of equal dose rate plotted as white contours. The logarithmic color scale for the dose rate is shown as the right scale in the figure; one step in color and the distance between neighboring lines of equal dose rate correspond to a factor of 2 in dose rate. The dose rate in μSv/hour is indicated on the labels attached to the white contours.

The electron beam interactions were modeled using the GEANT/DINREG MC routine [9] to generate vertices of electron and photon nuclear interactions and produce secondary neutrons. GEANT/CALOR tracked the hadronic cascades through the roof of the end station made of concrete and shielded by soil. The thickness of the dome-shaped roof was roughly equal to 2 m

of concrete. Biasing processes were adopted to increase by a factor of 2000 the neutron production cross section without perturbing the e, γ interactions, and also to amplify the hadronic cascade propagating through the roof by a factor of 64. The energy, direction, and coordinates of the outgoing neutrons were stored. The distribution of neutron exit coordinates is shown in the middle of Fig. 16 as a scatter plot. For each exiting neutron, the skyshine dose was calculated using the SKYD routine at every position of the map, and then added together. The resulting lines of equal dose show the azimuthally asymmetric skyshine dose distribution around the hall.

The asymmetry is caused, apart from the the original asymmetry of the problem, by the forward-peaked angular distribution of the secondary neutrons produced by the 4-GeV electron beam in the target and in the beam line.

The azimuthal direction of the maximum skyshine dose is determined by the coordinate, angular and energy distribution of neutrons entering air at the roof, which in turn depends on the angular and energy distribution of source neutrons and the variable effective thickness of roof shielding.

V. CONCLUSIONS

In conclusion, we used GCALOR Monte Carlo to calculate the skyshine dose distributions of neutrons and secondary photons as a function of such parameters as the distance from the neutron source from 0 up to 2 km, the energy of source neutrons ranging from thermal to 400 MeV, their emission angle from 0 to 90° from vertical, and the azimuthal difference between the neutron momentum direction and the direction from the source to the observation point. The results averaged over the azimuthal angle agree well with previous skyshine calculations. Strong azimuthal asymmetry of the skyshine dose at high neutron energies and at emission angles close to 90° makes the results of skyshine calculations in real environments, especially in the case of fixed target experiments at high-energy accelerators, sensitive to the assumption of the azimuthal symmetry of the neutron source. The parameterization formula and corresponding computer code have been developed which can be used for detailed calculations of the skyshine dose maps. The parameterization can be used both in analytical estimates of the skyshine doses and in Monte Carlo calculations where it helps to save essential computing time. The FORTRAN function SKYD and the parameter files are available upon request.

ACKNOWLEDGMENTS

[1] R. G. Alsmiller, Jr., J. Barish, and R. L. Childs, "Skyshine at neutron energies $\lesssim$ 400 MeV", Particle Accelerators, 11, 131 (1981).

[2] K. Hayashi and T. Nakamura, "Analytical Dose Evaluation Neutron and Secondary Gamma-Ray Skyshine from Nuclear Facilities", Nuclear Science and Engineering, 91, 332 (1985).

[3] G. Stapleton, K. O'Brien, R. Thomas, "Accelerator skyshine: Tyger Tyger Burning Bright", Particle Accelerators, 44, 1 (1994).

[4] G. Prabhakara Rao and P.K. Sarkar, "A Study of the Variation of Neutron Skyshine Dose with Respect to Roof Thickness, Source Spectrum Distribution", Journal of Testing and Evaluation, JTEVA, 23, No. 5, 388 (1995).

[5] C. Zeitnitz and T. A. Gabriel, "The GEANT - CALOR Interface User's Guide", (1995); C. Zeitnitz and T.A. Gabriel, "Status of the GEANT-CALOR interface", in: Proceedings of The Second Workshop on Simulating Accelerator Radiation Environments, CERN, 9-11 October 1995, CERN/TIS/RP/97-05, Geneva, Switzerland, February 1997, page 171.

[6] GEANT: Detector description and simulation tool, CERN Program Library entry W5013, CERN, Geneva, Switzerland (1994).

[7] U.S. Department of Energy. Occupational radiation protection. Final rule, 10 CFR 835, Federal Register 58(238), Part IV, Subpart A – General Provisions, §835.2 (b) Definitions; Washington, DC: Office of Health Physics and Industrial Hygiene Programs, 1993.

[8] MINUIT: Function minimization and error analysis, CERN Program Library entry D506, CERN, Geneva, Switzerland (1993).

[9] P. Degtyarenko, "Applications of the Photonuclear Fragmentation Model to Radiation Protection Problems", a presentation at the second specialist's meeting on Shielding Aspects of Accelerators, Targets and Irradiation Facilities (SATIF2), 12-13 October 1995, CERN, Geneva, Switzerland.